A Comparative Study between Vector Control and Direct Torque Control of Induction Motor Using Optimal Controller

Asst. Prof. Dr.Abdulrahim Thiab Humod , Asst. Prof. Dr. Mohammad Najm Abdullah , L. Fatma H. Faris

Abstract - This paper presents a comparison between two famous control strategies for induction motors: Field Oriented Control (FOC) and Direct Torque Control (DTC). These two strategies are Vector Control (VC) methods and provide a solution for high-performance drives. These strategies are implemented using an induction motor with ratings of 300W, 380V and 50Hz. The motor parameters are estimated using laboratory tests. From simulation results the advantages and disadvantages of both methods are investigated to illustrate the features of both methods. The performances of the two control schemes are evaluated in terms of torque, current ripples and transient responses to load toque variations.

The Space Vector Pulse Width Modulation (SVPWM) technique is proposed as a voltage source inverter. Also the Proportional Integral (PI) controller tuned by Particle Swarm Optimization (PSO) is proposed for both techniques. A MATLAB/SIMULINK program is prepared for simulating the overall drive systems.

Keywords - Field Oriented Control, Direct Torque Control, PI–PSO Based Controller, induction motor.

1 . INTRODUCTION:

The advantages of the Induction Motor (IM) includes high reliability, relatively simple, has rugged structure, low cost, robustness and high efficiencies. These advantages make the IM advance in all aspects like speed change, speed reversal, starting and braking. The overall system performance depends on the IM dynamic operation. Due to the swift development in microprocessor and power electronic, the advanced control methods have IM possible for high performance applications.

Variable frequency control techniques of IM can be divided into two major types: scalar control, vector control, Scalar control or as it is called V/f control assumes a constant relation between voltage and frequency and vector control. The first vector control method of induction motor was Field Oriented Control (FOC) presented by **K. Hasse** (Indirect FOC) and **F. Blaschke** (Direct FOC) in early of 1970s [1, 2], second vector control method of induction motor was Direct Torque Control (DTC) was first introduced by Takahashi in 1986. [3]

Many different studies have been developed to find out different solutions for induction motor control having the features of accuracy, quick torque response and reduction of the complexity of the presented algorithms and techniques, **Bendyk** [4] propose a DTC based on a High Frequency AC (HFAC) power converter, **Abdulrahim,** [5] propose a DTC based on Neuro fuzzy (ANFIS) controller to improve the performance of PI-PSO controller. ANFIS controller is trained by using PI-PSO data to improve the speed and torque response of three phase IM, **Turki**, [6] presented a method for improving the speed profile of a three phase induction motor in DTC drive system using a fuzzy logic based speed controller, **Abdesselam** [7] presents a comparative study of field oriented control and direct torque control of induction motors using an adaptive flux observer, **Supriya** [8] presents fuzzy logic based direct torque control (DTC) scheme of an induction motor (IM) and its comparative study using intelligent techniques under varying dynamic conditions are discussed, **Pabitra** [9] implemented of scalar & vector control of three phase induction motor drives, **Garcia** [10] presents a comparison between two control strategies FOC and DTC for permanent magnet synchronous motors, **A. Bennassar** [11] present the performance of the sensorless direct torque control (DTC) of an induction motor (IM) using adaptive Luenberger observer (ALO) with fuzzy logic controller (FLC) for adaptation mechanism.

2.MODELING AND SIMULATION OF THREE PHASE IM:

The per-phase equivalent circuit diagrams of an IM. in two- axis synchronously rotating reference frame are illustrated in figure (1). From the circuit diagram the following equations can be written [1].

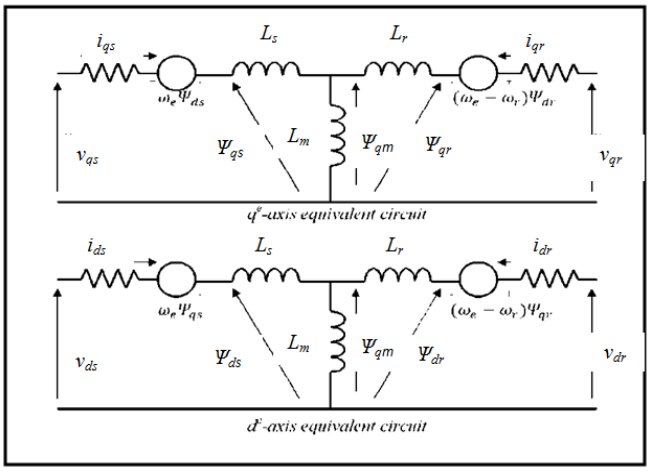

Fig. (1) $d^e - q^e$ I.M Equivalent Circuit

- Stator equation:

$$V_{qs}^{\ e} = R_s i_{qs}^{\ e} + \frac{d\Psi_{qs}}{dt} + w_e \Psi_{ds} \quad \ldots\ldots\ldots\ldots\ldots(1)$$

$$V_{ds}^{\ e} = R_s i_{ds}^{\ e} + \frac{d\Psi_{ds}}{dt} - w_e \Psi_{qs} \text{.....(2)}$$

● Rotor equation:

$$V_{qr}^{\ e} = R_r i_{qr}^{\ e} + \frac{d\Psi_{qr}}{dt} + (w_e - w_r)\Psi_{dr} \text{...(3)}$$

$$V_{dr}^{\ e} = R_r i_{dr}^{\ e} + \frac{d\Psi_{dr}}{dt} - (w_e - w_r)\Psi_{qr} \text{.....(4)}$$

Where: the superscript notation "e" referred to the synchronously rotating reference frame quantities.

It's obviously that in squirrel cage I.M Vqdr =0, then the pervious equation can be rewritten:

$$\frac{d\Psi_{qs}}{dt} = V_{qs}^{\ e} - R_s i_{qs}^{\ e} - w_e \Psi_{ds} \text{.....(5)}$$

$$\frac{d\Psi_{ds}^{\ e}}{dt} = V_{ds}^{\ e} - R_s i_{ds}^{\ e} + w_e \Psi_{qs} \text{.....(6)}$$

$$\frac{d\Psi_{qr}}{dt} = -R_r i_{qr}^{\ e} - (w_e - w_r)\Psi_{dr} \text{.....(7)}$$

$$\frac{d\Psi_{dr}}{dt} = -R_r i_{dr}^{\ e} + (w_e - w_r)\Psi_{qr} \text{.....(8)}$$

The development torque by interaction of air gap flux and rotor current can be found as:

$$Te = (3/2)\,(P/2)\,\overrightarrow{\Psi_m} \times \vec{I}_r \quad \text{.....(9)}$$

By resolving the variables into de-qe components:

$$Te = (3/2)\,(P/2)\,\left(\Psi_{ds} i_{qs}^{\ e} - \Psi_{qs} i_{ds}^{\ e}\right) \quad \text{.....(10)}$$

The dynamic torque equation of the rotor:

$$T_e = T_L + (\frac{2}{P}) J \frac{dw_r}{dt} \quad \text{.....(11)}$$

Where: ωr = is the rotor speed; P: no. of poles; J = rotor inertia; T_L= load torque.The stator current can be found by:

$$i_{ds}^{\ e} = \frac{\Psi_{ds} - \Psi_{dm}}{L_s} \quad \text{.....(12)}$$

$$i_{qs}^{\ e} = \frac{\Psi_{qs} - \Psi_{qm}}{L_s} \text{.....(13)}$$

The air gap flux

$$\Psi_{qm} = \frac{L_{m1}}{L_s}\Psi_{qs} + \frac{L_{m1}}{L_r}\Psi_{qr} \quad \text{.....(14)}$$

$$\Psi_{dm} = \frac{L_{m1}}{L_s}\Psi_{ds} + \frac{L_{m1}}{L_r}\Psi_{dr} \quad \text{.....(15)}$$

$$\text{Where: } L_{m1} = \frac{1}{(\frac{1}{L_m} + \frac{1}{L_s} + \frac{1}{L_r})} \text{....(16)}$$

From the previous equations the dynamic model of an induction motor is simulated as shown in figure (2).

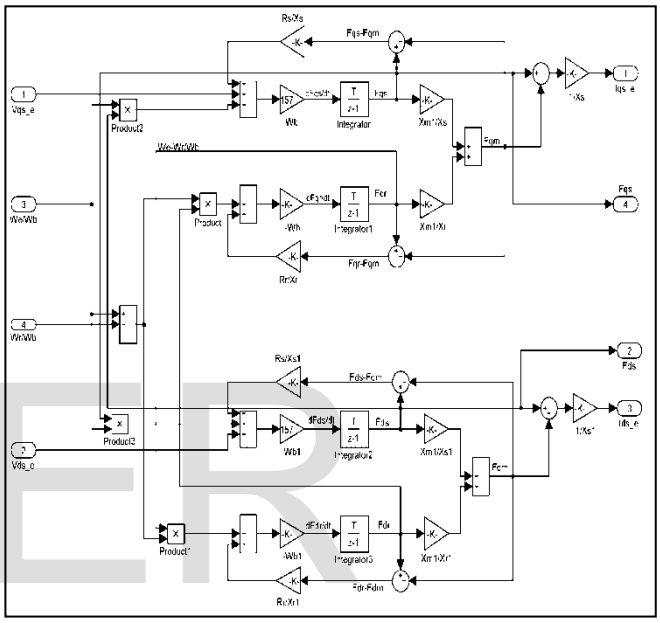

Fig. (2) IM Simulation

3 . VECTOR CONTROL OF INDUCTION MOTOR :

Vector control based on relations valid in dynamics state, not only magnitude and frequency but also instantaneous position of voltage, current and flux linkage space vector are controlled. The most popular vector control methods are the Field oriented control (FOC) and direct torque control (DTC).

3.1 Field-Oriented Control

Vector or Field-Oriented Control (FOC), allows a squirrel-cage induction motor to be driven with high dynamic performance. It transforms the dynamic structure of the A.C motor into that of separately excited D.C motor [1] , [2]. For D.C motor, the field flux is proportional to the field current, if the field assumed to be constant and independent of armature current, the armature current provides direct control torque, so that:

$$T_e \propto I_f * I_a \quad \text{.....(17)}$$

With the induction motor transformed to d-q plane, it looks like a separately excited D.C motor. The (FOC) technique decouples the two components of stator current;

one providing the air-gap flux, and the other producing the torque. These current components
provide independent control of flux and torque and the characteristic is linear [1] , [2] , [12]. These components are transferred back to the stator frame before feeding back to the rotor. The two components are d-axis i^s_{ds} analogues to field current I_f, and q-axis i^s_{qs} is analogues to armature current I_a of the separately excited D.C motor [1] , [2] , [12]. This strategy can be implemented by align the rotor flux vector along the d-axis of the stationary frame as shown by the phasor diagram in figure (3). The fundamentals of vector control implementation can be explained in figure (4), where the motor model is presented in a synchronously rotating reference frame, the voltage-fed SPWM inverter produces three-phase voltages (v_a, v_b, v_c) according to the reference command voltages (v^*_a, v^*_b, v^*_c) the flux component of stator current (i^{s*}_{ds}) and the torque component of the stator current (i^{s*}_{qs}) is used as a control signals to the system, which are inversely transformed to three-phase reference currents (i^*_a, i^*_b, i^*_c), and then transferred to three-phase voltages (v^*_a, v^*_b, v^*_c) through (PI) controller [1] , [2]. The vector control FOC can be implemented by either direct or indirect method, these methods are different essentially by how the unit vector ($\cos\theta_e$ and $\sin\theta_e$) is estimated for the controller.

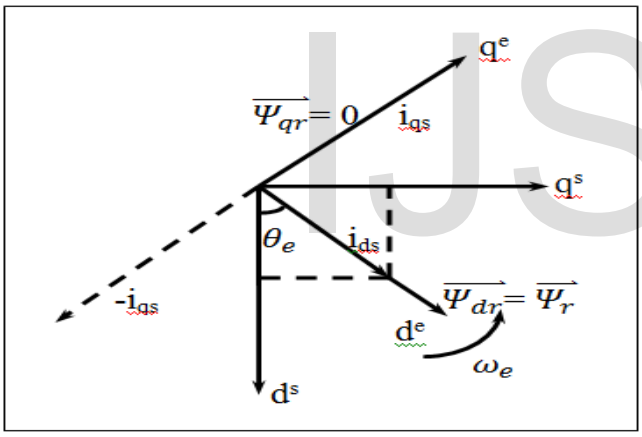

Fig. (3) Correct Rotor Flux Orientation

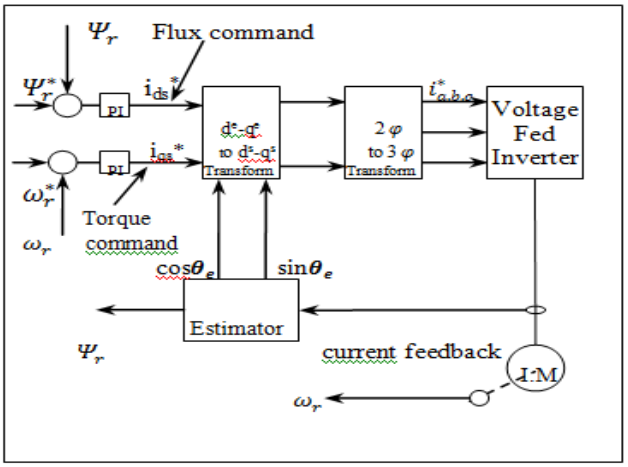

Fig. (4) Field Oriented Vector Control

3.1.1 Flux Vector Estimation:

There are two commonly methods of flux estimation; voltage model, and current model. The first one has strong performance in high speed regions but not in low speeds. Whereas, the second method has an accepted performance in both low and high speeds [1].

The current model depends on the main rotor equations in the two axes stationary frame ds-qs, superscript "s" referred to stationary frame quantities:

$$R_r i_{qr}{}^s + \frac{d\Psi_{qr}{}^s}{dt} - w_r \Psi_{dr}{}^s = 0 \quad \text{.....(18)}$$

$$R_r i_{dr}{}^s + \frac{d\Psi_{dr}{}^s}{dt} + w_r \Psi_{qr}{}^s = 0 \quad \text{.....(19)}$$

Adding terms $(LmRr/Lr)\, i^s_{ds}$ and $(LmRr/Lr)\, i^s_{qs}$ and simplifying, get:

$$\Psi^s_{qr} = \int [\frac{Lm}{Tr} i^s_{qr} + \omega_r \Psi^s_{dr} - \frac{\Psi^s_{qr}}{Tr}] \dots\dots\dots (20)$$

$$\Psi^s_{dr} = \int [\frac{Lm}{Tr} i^s_{dr} - \omega_r \Psi^s_{qr} - \frac{\Psi^s_{dr}}{Tr}] \dots\dots\dots (21)$$

Where: $Tr = \frac{Lr}{Rr}$ is the rotor time constant.

Equations (20 & 21) give rotor fluxes as a function of stator currents and speed. Therefore, knowing these signals, the rotor flux and corresponding unit vector ($\cos\theta_e$ and $\sin\theta_e$) can be estimated by means of DSP microprocessor to implement the following equations [1] , [2]:

$$\left.\begin{aligned} \overrightarrow{\Psi_r} &= \sqrt{\Psi^{s2}_{qr} + \Psi^{s2}_{dr}} \\ \Psi^s_{qr} &= \overrightarrow{\Psi_r} \sin\theta_e \\ \Psi^s_{dr} &= \overrightarrow{\Psi_r} \cos\theta_e \\ \text{Or: } \sin\theta_e &= \frac{\Psi^s_{qr}}{\overrightarrow{\Psi_r}} \\ \cos\theta_e &= \frac{\Psi^s_{dr}}{\overrightarrow{\Psi_r}} \end{aligned}\right\} \dots\dots(22)$$

Flux estimation by the current model requires a speed encoder, but the advantage is that the drive operation can be extended down to low and zero speed. It's important to mention, that the input signals to the estimator (i^s_{qs} and i^s_{ds}) must be filtered by a low pass filter stage. The simulation of the current model estimator can be shown in figure (5).

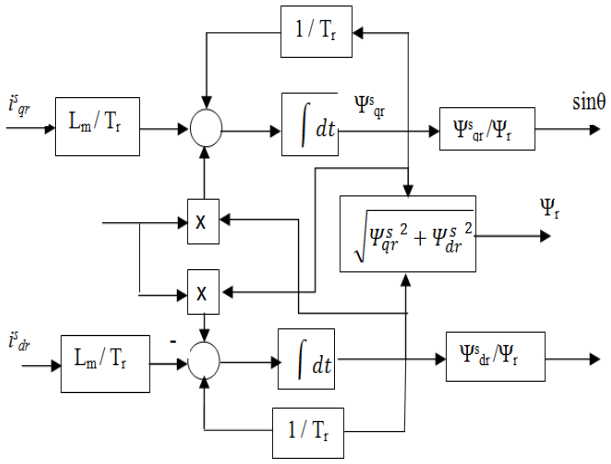

Fig. (5) Current Model Flux Estimation

3.2 Direct Torque Control (DTC)

Direct Torque Control describes the way in which the control of torque and speed are directly based on the electromagnetic state of the motor, similar to a DC motor, but contrary to the way in which traditional PWM drives use input frequency and voltage. Direct torque control is the first technology to control the "real" motor controlled variables as torque and flux [13]. The basic principle in conventional DTC for IM is to directly select stator voltage vectors by means of a hysteresis stator flux and torque control as in Fig.(6) .

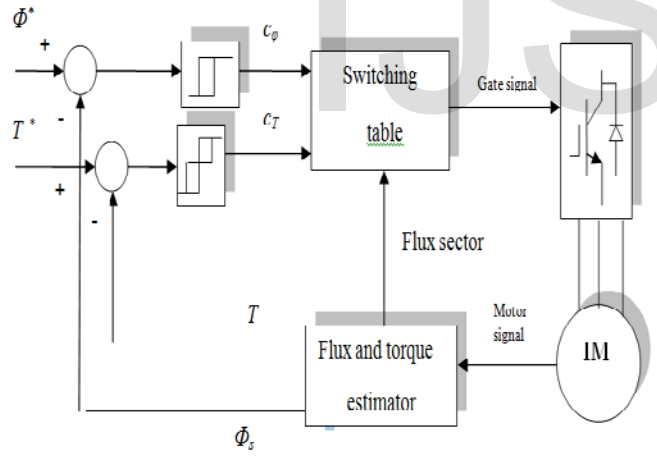

Fig. (6) DTC block diagram

From this figure stator flux Ψs* and torque Ts* are compared with the corresponding estimated values. Both stator flux and torque errors are processed by means of hysteresis band comparators. In particular, stator flux is controlled by a two level hysteresis comparator, whereas the torque is controlled by a three level comparator. On the basis of the hysteresis comparators and stator flux sector a proper VSI voltage vector is selected by means of the switching table given in Table 1.

Table (1)
Switching Table of inverter

H_ψ	H_{Te}	S(1)	S(2)	S(3)	S(4)	S(5)	S(6)
1	1	V_2	V_3	V_4	V_5	V_6	V_1
	0	V_0	V_7	V_0	V_7	V_0	V_7
	-1	V_6	V_1	V_2	V_3	V_4	V_5
0	1	V_3	V_4	V_5	V_6	V_1	V_2
	0	V_7	V_0	V_7	V_0	V_7	V_0
	-1	V_5	V_6	V_1	V_2	V_3	V_4

Generally, in a symmetrical three phase induction motor, the instantaneous electromagnetic torque is proportional to the cross product of the stator flux linkage space vector and the rotor flux linkage space vector [14].

$$T_e = \left(\frac{3p}{2}\right) \psi_s \psi_r \sin\delta) \quad \ldots\ldots\ldots (23)$$

Where ψ_s , is the stator flux linkage space vector , ψ_r is the rotor flux linkage space vector referred to stator and (δ) is the angle between the stator and rotor flux linkage space vectors.

The estimator equations for stator flux (ψs), stator flux position(θs)and torque are:

$$\psi_s = \sqrt{\psi_{qs}{}^2 + \psi_{ds}{}^2} \ldots\ldots\ldots\ldots\ldots\ldots (24)$$

$$\theta_s = \tan^{-1}\left(\frac{\psi_{qs}}{\psi_{ds}}\right) \ldots\ldots\ldots\ldots\ldots\ldots (25)$$

$$T_e = \left(\frac{3p}{2}\right) (\psi_{ds} i_{qs} - \psi_{qs} i_{ds}) \ldots\ldots\ldots\ldots\ldots (26)$$

4. Particle Swarm Optimization (PSO)

The PSO algorithm is one of the optimization techniques developed by Eberhart and Kennedy in 1995. This method has been found to be robust in solving problems featuring non-linearity and non-differentiability, which is derived from the social-psychological [15]. It was inspired by the social behavior of bird flocking and fish schooling, and has been found to be robust in solving continuous nonlinear optimization problems. PSO becomes a focus these days due to its simplicity and ease to implement [16].

In PSO, each single solution is a "bird" in the search space; this is referred to as a "particle". The swarm is modeled as particles in a multidimensional space, which have positions and velocities. These particles have two essential capabilities: their memory of their own best position and knowledge of the global best position. Members of a swarm communicate good positions to each other and adjust their own position and velocity based on good positions [16]. The particles are updated according to the following equations (27 & 28).

$$v(k+1)_{i,j} = w.v(k)_{i,j} + c_1 r_1 (gbest - x(k)_{i,j}) + c_2 r_2 (pbest_j - x(k)_{i,j}) \quad \ldots . (27)$$

$$x(k+1)_{i,j} = x(k)_{i,j} + v(k)_{i,j} \quad \ldots\ldots\ldots\ldots\ldots (28)$$

Where,

$v_{i,j}$: velocity of particle i and dimension j.

$x_{i,j}$: position of particle i and dimension j.

c_1, c_2 : known as acceleration constants.

w : inertia weight factor.

r_1 , r_2 : random numbers between 0 and 1.

pbest : best position of a specific particle.

gbest : best particle position of the group.

4.1 Performance criteria of PSO-PI controller

In most intelligent optimization algorithms, there are commonly performance criteria such as: Integrated Absolute Error (IAE), the Integrated of Square Error (ISE), and Integrated of Time Square Error (ITSE). That can be evaluated analytically in frequency domain. These performance criteria are including the overshoot, rise time, settling time and steady-state error. In addition, it has been indicated the optimization, and robust of the drive system .The performance criterion formulas are as follows[15]:

Integral Square Error

$$(ISE) = \int_0^\infty e^2(t).dt \quad \ldots\ldots\ldots\ldots (29)$$

Integral Absolute Error

$$(IAE) = \int_0^\infty |e(t)|.dt \quad \ldots\ldots\ldots\ldots (30)$$

Integral Time Square Error

$$(ITSE) = \int_0^\infty t.e^2(t).dt \quad \ldots\ldots\ldots\ldots (31)$$

In this paper the (ITSE) time domain criterion is used as a "fitness function" for evaluating the PI controller performance. A set of good controller parameters K_p and K_i can yield a good step response that will result in performance criteria minimization.

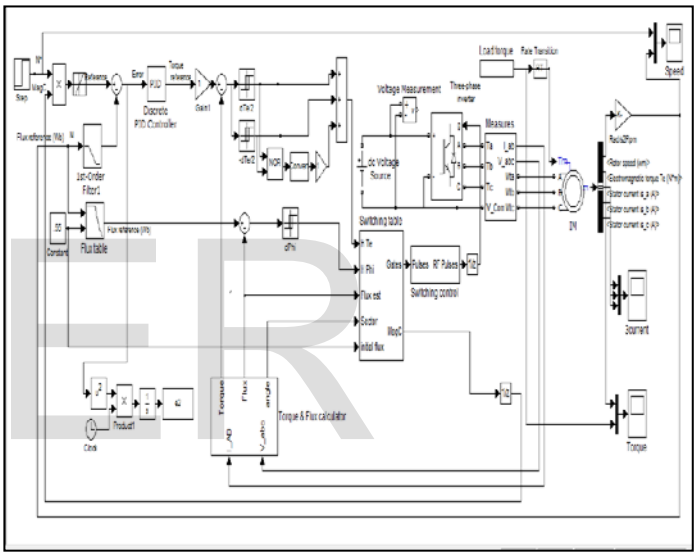

5. Simulation and Results

Each of the two control schemes are simulated using MATLAB/Simulink. The inputs to the simulation model are the applied voltage and rotor speed. Then the model calculates the stator current, stator flux, rotor current, rotor flux, and torque.The values of the electrical design parameters for 3-phase squirrel cage IM used in the simulation are shown in the appendix A and the look up table that used for optimum switching states is shown in table (1) . Figures (7) and (8) shows the MATLAB/ Simuink circuit of FOC and DTC.

Swarm size (Number of birds)	10
Number of iterations	**30**
Cognitive coefficient (C_1)	1.2
Social coefficient (C_2)	1.2
Inertia weight (w)	0.3

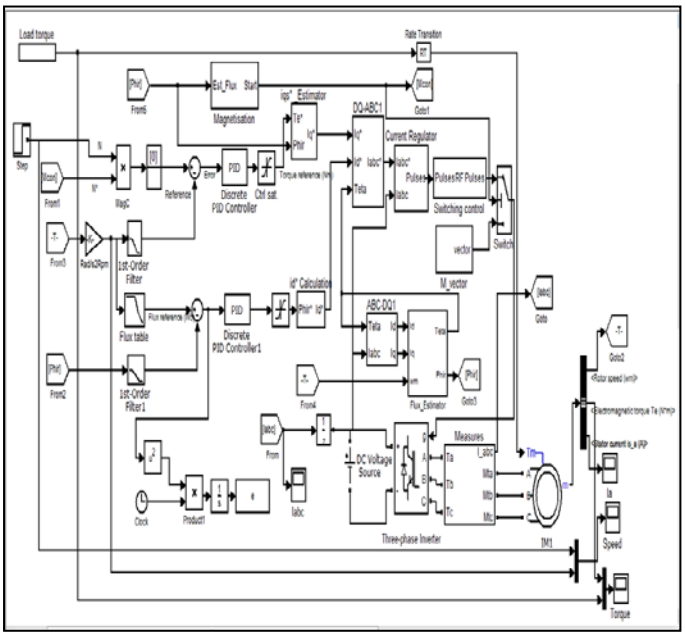

Fig. 7. FOC with PI-PSO Matlab/Simulink circuit

Fig. 8. DTC with PI-PSO Matlab/Simulink circuit

The PSO tuning method in this work depends on ITSE performance index. The parameters of PSO algorithm that achieve better solution are listed in table (2).

Comparison criterion	FOC	DTC
Dynamic response	Quicker	Slower
Torque ripple	Low	High
Parameter sensitivity	Decoupling depends on Lsd, Lsq ,Lm ,Lr	For a sensorless estimator: Rs
Requirement of rotor position	Yes	NO
Coordinate transformation	Yes	NO
Complexity and processing requirements	Higher	Lower
Control tuning	PI gains	Hysteresis bands and PI
General	Good	Good

Table (2)
PSO parameters

The responses of the speed and torque for FOC and DTC with PI- controller tuned by PSO technique at different loads and speeds conditions . Where the selected speeds are (3000 ,1500 , 100 , 10) r.p.m. , for load torques are (0 , 0.5 , 1) N.m. . The obtained gains of PI-PSO technique for FOC are [(kp = .7287 , ki = 4.0743) for PI of flux controller , (kp = 3.3665 , ki = 2.4073) for PI of torque controller)] and for DTC (kp=1.1666 , ki=4.3455) .

Figures (9,10,11,12,) show the speed response for above values of speed for no load at (0 - 0.8) sec , 0.5 N.m. at (0.8 – 1.2) sec and 1 N.m. at (1.2 – 2) sec .

The speed response for FOC show peak to peak ripple values (0.04 , 0.03 , 0.02 , 0.01) r.p.m and the percentage values for ripple (0.0013% , 0.002% , 0.02% , 0.1%) respectively for above speeds while DTC show peak to peak ripple values (0.4 , 0.3 , 0.2 , 0.1) r.p.m. and the percentage values of ripple (0.01% , 0.02% , 0.2% , 1%) .This results shows that the speed response for DTC has ripple more than FOC .

The overshoot in the speed response for FOC are (4% , 6.3% , 31% , 35%) and undershoot at applied loads is (65%) respectively for above speeds while DTC are (2.3% , 2.6% , 23% , 25%) and undershoot is (30%) .

Figures (13,14,15,16) show the torque response for above speed values for no load at (0 - 0.8) sec , 0.5 N.m. at (0.8 – 1.2) sec and 1 N.m. at (1.2 – 2) sec .

The starting torque for FOC equal (7.3 , 7.2 , 5.3 , 0.65) N.m respectively for above speeds while DTC equal (7 , 6.8 , 6.5 , 1.4) N.m .

The torque response for FOC has peak to peak ripple values (0.12 , 0.1 , 0.09 , 0.04) N.m. respectively for above speeds while DTC has peak to peak ripple values (0.46 , 0.5 , 0.9 , 0.7) N.m. The torque response for DTC has ripple more than FOC .

Figures (17,18,) show the speed and torque response for FOC and DTC at different speeds for ramp input with slop (0.2 sec), this figures shows that the starting torque value for FOC less than DTC .

6. Conclusion

This paper presents a comparison between two torque control methods for induction motor drive. The description of two control schemes and their principle of operation have been presented. DTC was developed as an alternative to FOC that had been in use for a number of years, it can be shown that the FOC algorithm provides faster response than DTC. FOC has lower ripple than DTC in the speed and torque responses especially at low speeds. The torque ripple in DTC has no significant effect on the speed response . The comparison between two methods of control shown in table (3) .

TABLE 3
comparative between FOC and DTC of IM

REFERENCES

[1] Bimal K. Bose, "Modern Power Electronic and AC Drives", Prentice Hall, 2002.
[2] Qusay L. Hamdi, "Design of Indirect Field-Oriented PWM Inverter for Three-Phase Induction Motor", Ph.D. Thesis, Al-Rasheed collage of engineering, University of Technology, 2007.
[3] I.Takahashi and Y.Ohmori, High-performance direct torque control of an induction motor, IEEE Transactions on Industrial Applications, vol.25: 257-264, 1989.
[4] M. Bendyk, P. C. K. Luk, P. Jinupun," Direct Torque Control of Induction Motor Drives Using High Frequency Pulse Density Modulation for

Reduced Torque Ripples and Switching Losses", IEEE, Power Electronics Specialists Conference (PESC), 17-21 June, 2007. pp. 86-91

[5] Dr. Abdulrahim T. Humod , Wiam I. Jabbar , " Direct Torque Control of an Induction Motor Based on Neurofuzzy " Eng. & Tech. Journal, Vol. 31,Part (A), No. 17, 2013. Eng. &Tech. Journal, Vol.

[6] Turki Y. Abdalla, Haroution Antranik Hairik and Adel M. Dakhil," Minimization of Torque Ripple in DTC of Induction Motor Using Fuzzy Mode Duty Cycle Controller", Iraq J. Electrical and Electronic Engineering, Vol. 7 No. 1, 2011.

[7] Abdesselam Chikhi1,a), Mohamed Djarallah1,b), Khaled Chikhi1,c) ," A Comparative Study of Field-Oriented Control and Direct-Torque Control of Induction Motors Using An Adaptive Flux Observer" , Serbian Journal Of Electrical Engineering Vol. 7, No. 1, May 2010.

[8] Supriya More and Anant Kulkarni ," Direct Torque Control of Induction Motor Using Fuzzy Logic Controller " IOSR Journal of Electrical and Electronics Engineering (IOSR-JEEE) e-ISSN: 2278-1676,p-ISSN: 2320-3331, Volume 10, Issue 5 Ver. I PP 53-61, Sep – Oct. 2015 .

[9] Pabitra Kumar Behera1, Manoj Kumar Behera2, Amit Kumar Sahoo3, " Comparative Analysis of scalar & vector control of Induction motor through Modeling &Simulation " , International Journal Of Innovative Research In Electrical, Electronics, Instrumentation And Control Engineering Vol. 2, Issue 4, April 2014.

[10] X. T. Garcia1, B. Zigmund2, A. Terlizzi3,R. Pavlanin2, L. Salvatore3 , " Comparison Between Foc And Dtc Strategies For Permanent Magnet Synchronous Motors " Advances in Electrical and Electronic Engineering.

[11] A. Bennassar*, A. Abbou, M. Akherraz, M. Barara , " Fuzzy Logic Based Adaptation Mechanism For adaptive Luenberger Observer Sensorless Direct Torque Control Of Induction Motor " Journal of Engineering Science and Technology Vol. 11, No. 1 , 2016 .

[12] S.K. Pillai, "A First Course on Electrical Drives", second edition, 1989.

[13] S Allirani, V Jagannathan, "High Performance Direct Torque Control of Induction Motor Drives Using Space Vector Modulation" IJCSI, Vol. 7, Issue 6, November 2010.

[14] Ali Hussein Numan, "Speed and Position Sensorless Vector Control of Hybrid Stepper Motor Using Extended Kalman Filter", Department of Electromechanical Engineering, University of Technology, Baghdad, Iraq , Ph.D. Thesis, May, 2009.

[15] Fadhil A. Hassan and Lina J. Rashad," Particle Swarm Optimization for Adapting Fuzzy Logic Controller of SPWM Inverter Fed 3-Phase IM", Eng. & Tech. Journal, Vol. 29, No. 14, 2011.

[16] Y. Yan - W.A. Klop and M. Molenaar - P. Nijdam, " Tuning a PID controller: Particle Swarm Optimization versus Genetic Algorithms", February 2010.

APPENDIX:

1 - Induction motor data

Rated power 300 W
Rated voltage 380 V
Rated frequency 50 Hz
Rated speed 3000 rpm
Number of poles 2
Stator resistance Rs = 15.3 Ω
Stator inductance Ls = 0.038 H
Rotor resistance Rr =11.7 Ω
Rotor inductance Lr = 0.0288 H
Mutual inductance Lm = 0.75 H
Moment of inertia 0.0173 Kg.m2 /sec

FOC **DTC**

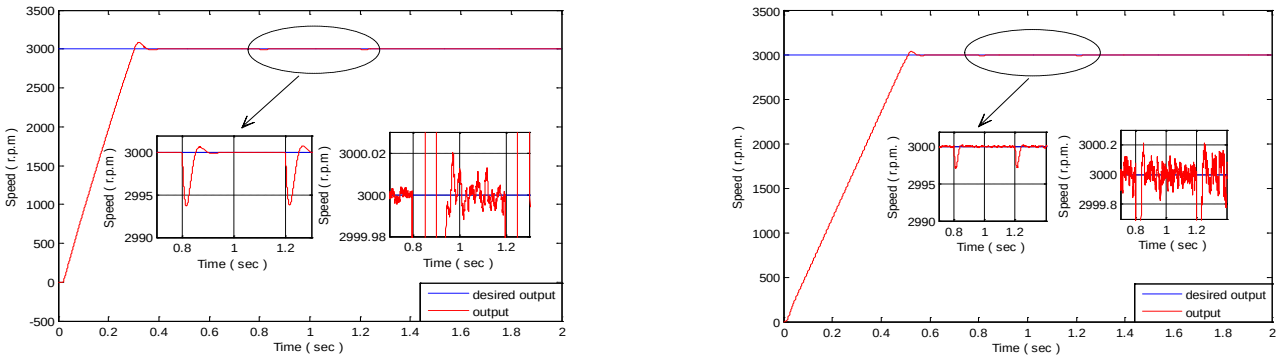

Fig. 9. Speed response for N=3000 r.p.m.

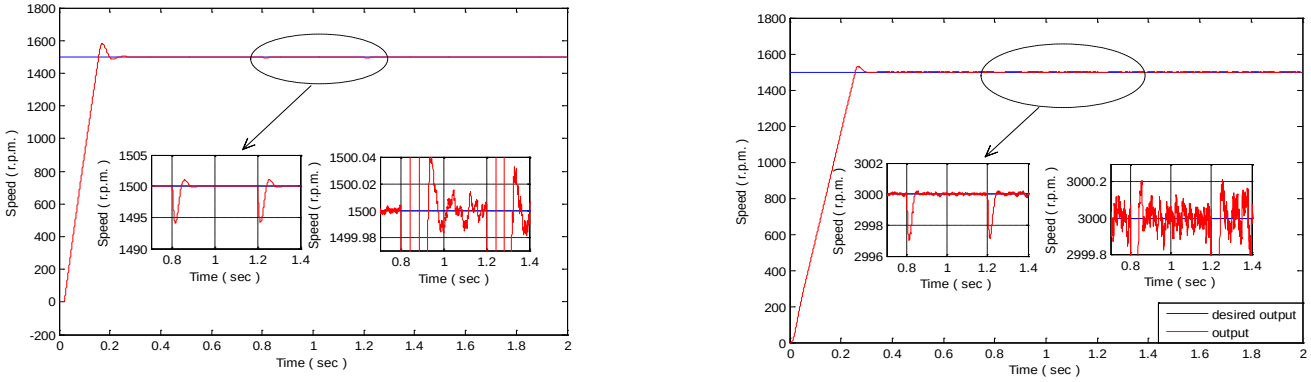

Fig. 10. Speed response for N = 1500 r.p.m.

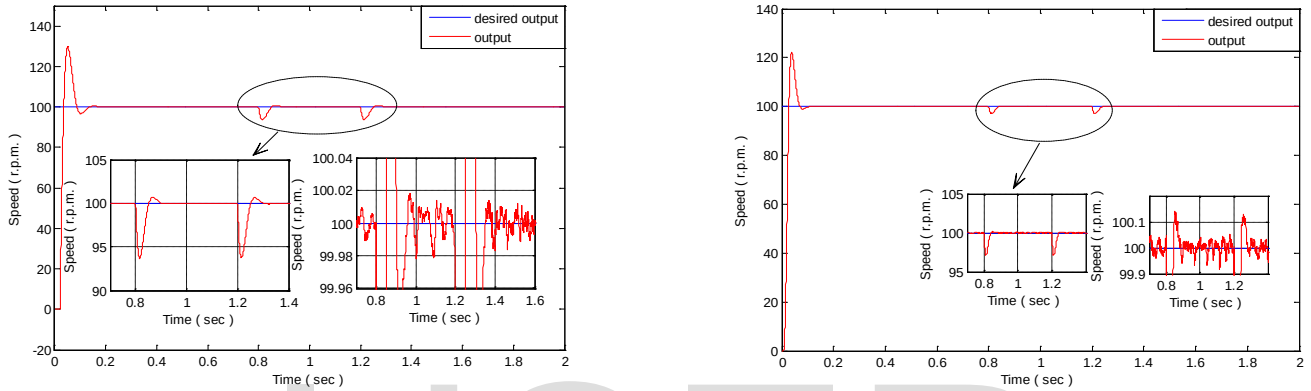

Fig. 11. Speed response for N= 100 r.p.m.

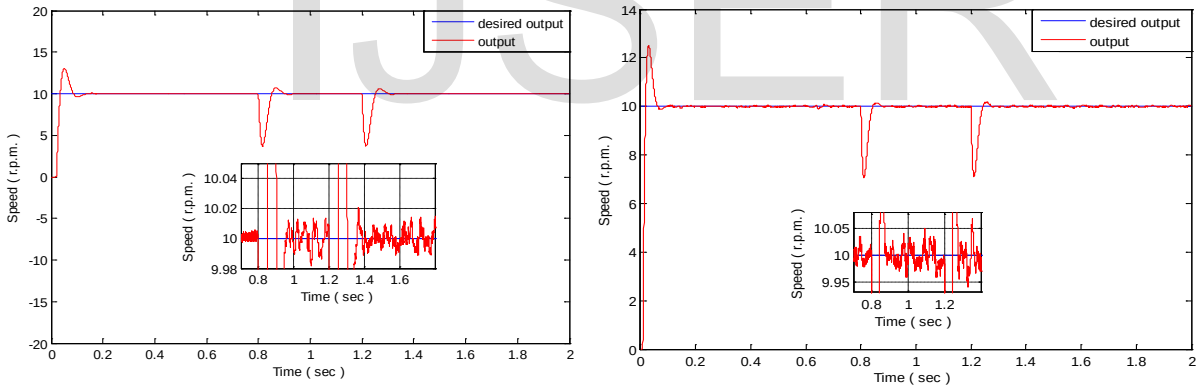

Fig. 12. Speed response for N = 10 r.p.m.

FOC **DTC**

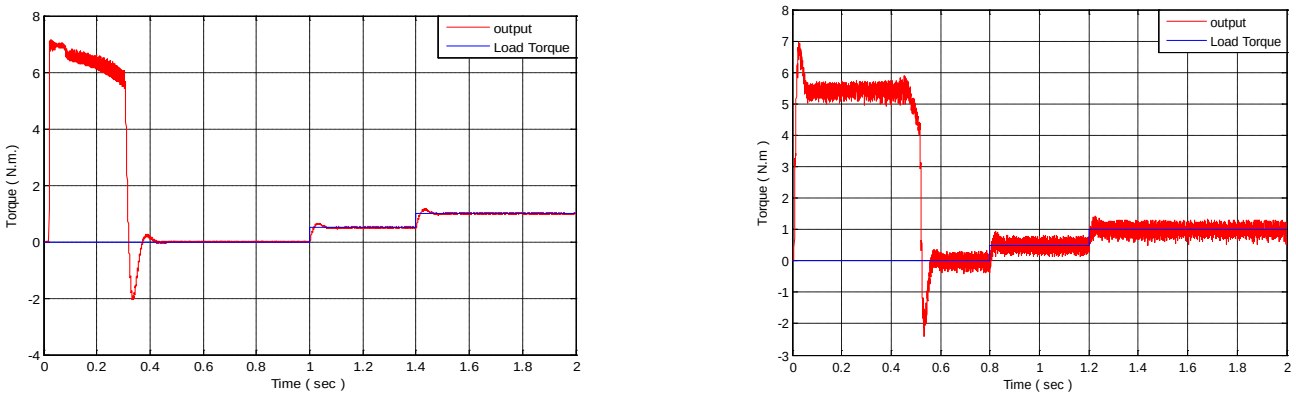

Fig. 13. Torque response at N = 3000 r.p.m.

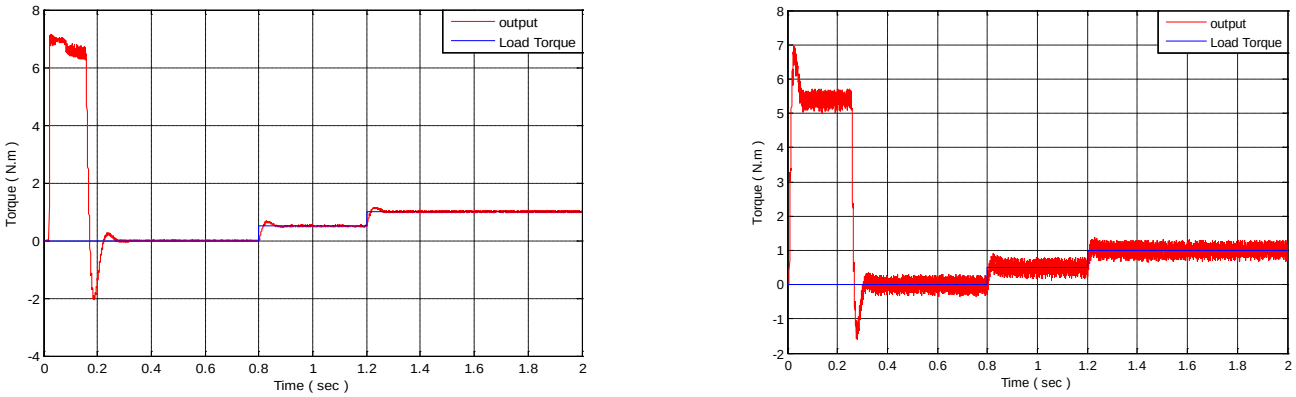

Fig. 14. Torque response at N = 1500 r.p.m.

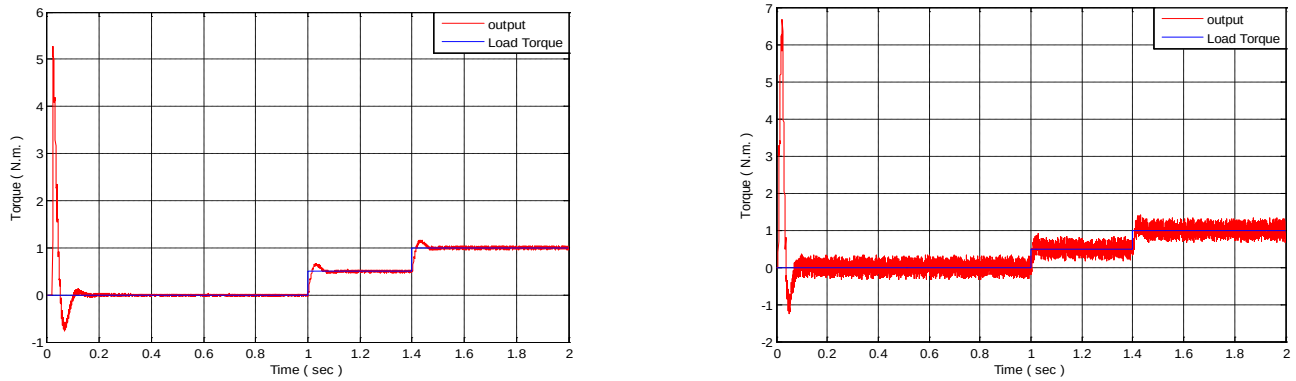

Fig. 15. Torque response at N = 100 r.p.m.

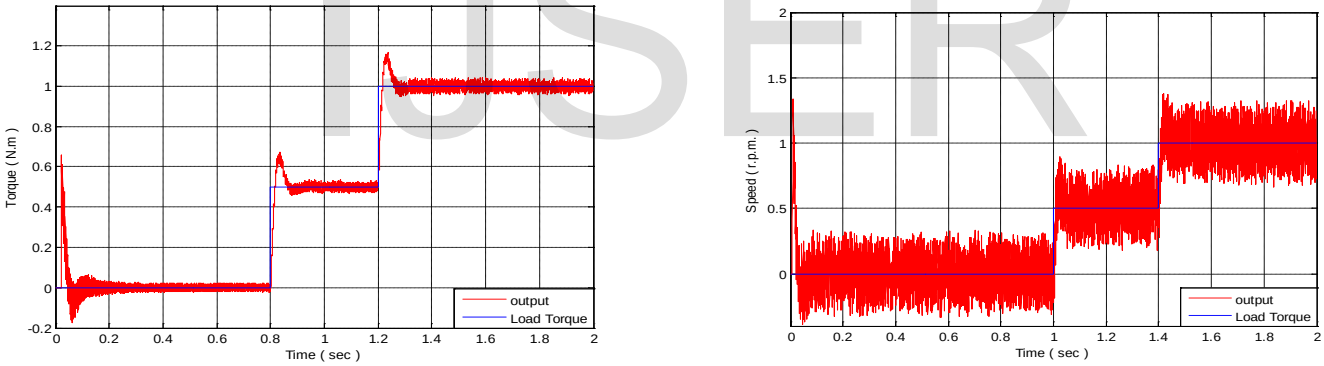

Fig. 16. Torque response at N = 10 r.p.m.

FOC **DTC**

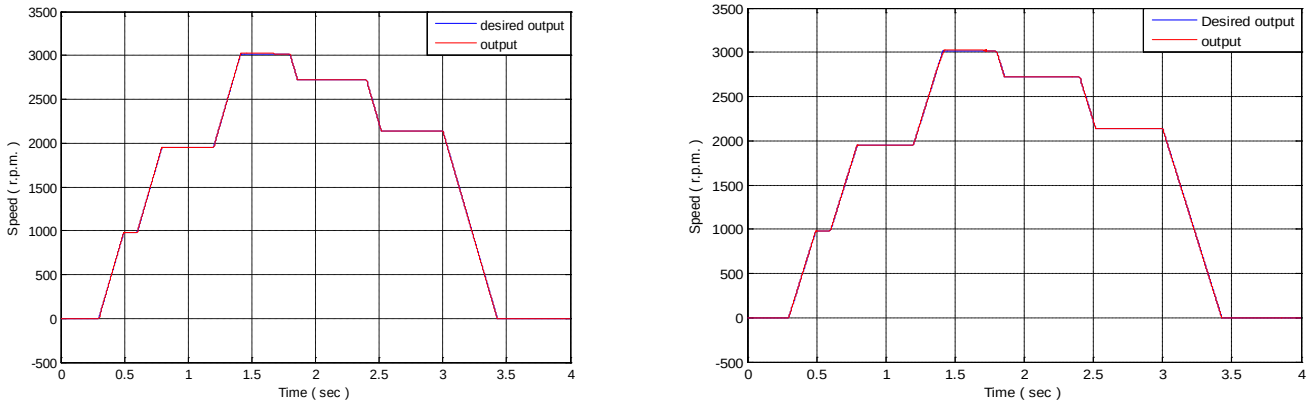

Fig. 17. Speed response at different values

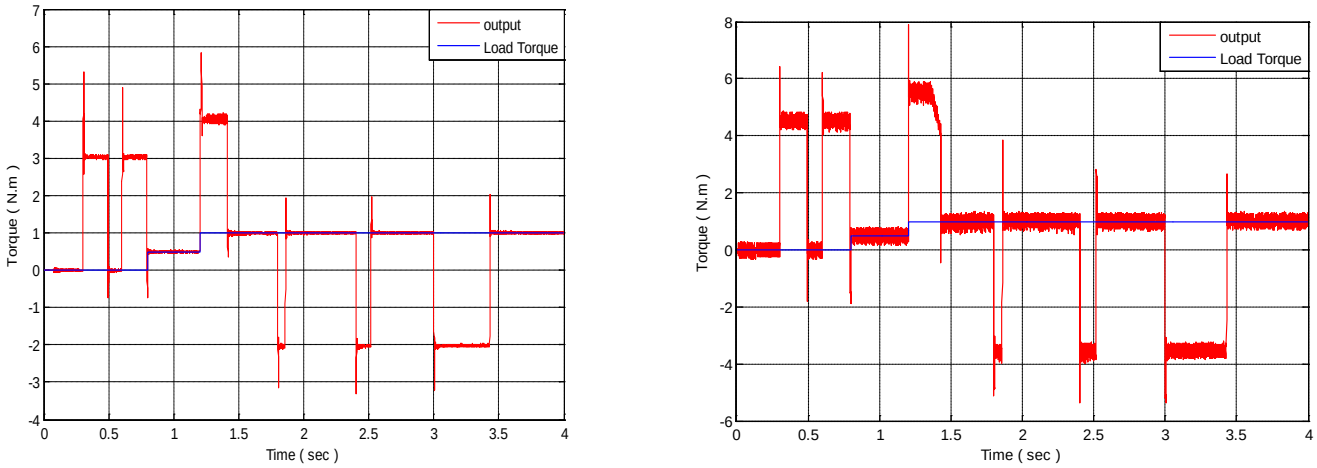

Fig. 18. Torque response at different speed